Title

Wet—dry cycles cause nucleic acid monomers to polymerize into long chains

Journal

Proceedings of the National Academy of Sciences of the United States of America, 121(49)

ISSN

0027-8424

Authors

Song, Xiaowei

Simonis, Povilas

Deamer, David

et al.

Publication Date

2024-12-03

DOI

10.1073/pnas.2412784121

PNAS RESEARCH ARTICLE | CHEMISTRY EVOLUTION

Wet–dry cycles cause nucleic acid monomers to polymerize into long chains

Xiaowei Song[a,1], Povilas Simonis[b,c,d,1], David Deamer[b,2], and Richard N. Zare[a,2]

Contributed by Richard N. Zare; received June 25, 2024; accepted October 23, 2024; reviewed by Veronica Vaida and Sidney Becker

The key first step in the oligomerization of monomers is to find an initiator, which is usually done by thermolysis or photolysis. We present a markedly different approach that initiates acid-catalyzed polymerization at the surface of water films or water droplets, which is the reactive phase during a wet–dry cycle in freshwater hot springs associated with subaerial volcanic landmasses. We apply this method to the oligomerization of different nucleic acids, a topic relevant to how it might be possible to go from simple nucleic acid monomers to long-chain polymers, a key step in forming the building blocks of life. It has long been known that dehydration at elevated temperatures can drive the synthesis of ester and peptide bonds, but this reaction has typically been carried out by incubating dry monomers at elevated temperatures. We report that single or multiple cycles of wetting and drying link mononucleotides by forming phosphodiester bonds. Mass spectrometric analysis reveals uridine monophosphate oligomers up to 53 nucleotides, with an abundance of 35 and 43 nt in length. Long-chain oligomers are also observed for thymidine monophosphate, adenosine monophosphate, and deoxyadenosine monophosphate after exposure to a few wet–dry cycles. Nanopore sequencing confirms that long linear chains are formed. Enzyme digestion shows that the linkage is the phosphodiester bond, which is further confirmed by ^{31}P NMR and Fourier transform infrared spectroscopy. This suggests that nucleic acid oligomers were likely to be present on early Earth in a steady state of synthesis and hydrolysis.

Oligomerization | nucleic acids | nanopore sequencing | wet-dry cycles | prebiotic chemistry

Significance

Evidence is presented that nucleic acid monomers can be transformed into long-chain polymers by wet–dry cycles simulating processes that are ubiquitous in hot spring sites associated with volcanic activity. These results come from analysis based on mass spectrometry and nanopore sequencing of monomeric samples that have been subjected to wet–dry cycling. This work addresses the question of how RNA and DNA might have first emerged in the history of life on Earth when no enzymes were available to catalyze their formation.

For life to begin on the prebiotic Earth, there must have been a nonenzymatic process capable of driving condensation reactions required for the synthesis of polymers resembling nucleic acids. Earlier studies using chemically activated mononucleotides have demonstrated that oligomers can be spontaneously assembled from nucleotides. For instance, Inoue and Orgel (1) reported that the imidazole ester of guanosine monophosphate assembles on a polycytidylic acid template and polymerizes into short oligomers of RNA. Ferris (2) discovered that the imidazole ester of adenosine monophosphate (AMP) in the presence of montmorillonite clay formed oligomers of polyadenylic acid. More recently, 2′-3′ cyclic guanosine monophosphate has been shown to spontaneously polymerize (3), and Obianyor et al. (4) investigated nonenzymatic DNA ligation in which carbodiimide was used as a phosphate activating agent. See Krishnamurthy and Hud (5) for review. These results depend on the assumption that monomers must be chemically activated to cause polymerization. However, there has been no consensus on a plausible prebiotic activation process. We present evidence that wet–dry cycles could have provided the needed activation for the formation of nucleic acid polymers.

Wet–dry cycles are ubiquitous in freshwater hot springs associated with subaerial volcanic landmasses. In previous studies, Ross and Deamer (6, 7) explored the thermodynamic and kinetic properties of such cycles and concluded that evaporation provides an increasingly significant air/water interface that, as discussed below, emerges as a foundational factor in oligomer growth. The present manuscript describes tests of the hypothesis that wet–dry cycles could drive nonenzymatic nucleic acid synthesis in the prebiotic environment without chemical activation. Here, we report that a single or just a few cycles of wetting and drying link mononucleotides by ester bonds to form polymers ranging from tens to hundreds of nucleotides in length. The resulting products were analyzed by nanoelectrospray ionization mass spectrometry (nESI–MS) and nanopore sequencing. MS identified multiple species of oligomers in the mixture of products. For instance, nESI–MS identified uridine monophosphate (UMP) oligomers 35 and 43 nucleotides in length. Oligomeric products were also observed when thymidine monophosphate, adenosine monophosphate, and deoxyadenosine monophosphate were exposed to wet–dry cycles. Nanopore sequencing confirmed that the polymers are linear polyanion chains linked by phosphodiester linkages. The implications of these findings bear directly on how it might be possible for one of the fundamental polymers of life to emerge on the prebiotic Earth.

Author affiliations: [a]Department of Chemistry, Stanford University, Stanford, CA 94305; [b]Department of Biomolecular Engineering, University of California, Santa Cruz, CA 95064; [c]Institute of Chemistry, Faculty of Chemistry and Geosciences, Vilnius University, Vilnius LT-01513, Lithuania; and [d]State Research Institute Center for Physical Sciences and Technology, Vilnius LT-02300, Lithuania

Author contributions: D.D. and R.N.Z. designed research; X.S. and P.S. performed research; X.S., P.S., D.D., and R.N.Z. analyzed data; and X.S., P.S., D.D., and R.N.Z. wrote the paper.

Reviewers: V.V., University of Colorado Boulder; and S.B., Max-Planck-Institut fur molekulare Physiologie Abteilung Chemische Biologie.

Competing interest statement: Baltic-American Freedom Foundation (BAFF) and Research Council of Lithuania (LMTLT), agreement No. S-PD-24-69; US Air Force Office of Scientific Research through the Multidisciplinary University Research Initiative program (AFOSR FA9550-21-1-0170).

[1]X.S. and P.S. contributed equally to this work.

[2]To whom correspondence may be addressed. Email: deamer@soe.ucsc.edu or rnz@stanford.edu.

This article contains supporting information online at https://www.pnas.org/lookup/suppl/doi:10.1073/pnas.2412784121/-/DCSupplemental.

Published November 25, 2024.

Results

MS Identification. MS analysis confirms that a nucleotide polymerization process can be driven by wet–dry cycling. For each length of the nucleotide polymer chain, multiple associated ion clusters were detected in the MS spectrum (*SI Appendix*, Fig. S1). The chemical information and relationship among these clusters can be established based on their relative mass-to-charge (m/z) differences as described in the methods section (*SI Appendix*, Fig. S2). Taking a mass spectrum from uridylic acid as a typical example, the $\Delta(m/z)$ of approximately 0.25 between isotope peaks indicated that the oligomer carried 4 charges. The $\Delta(m/z)$ of approximately 4.5 and 5.5 indicated the attachment of one water molecule and one sodium ion to the oligomer. For example, given the charge number (z) of 4 and a value of $\Delta(m/z)$ = 5.5 between 3329.3 and 3323.8, it can be known that an additional H atom from the polymer was replaced with a sodium atom (Na-H, mass = 5.5 × 4 = 22 Da). Similarly, according to $\Delta(m/z)$ value of 9.0 between 3332.8 and 3323.8, it can be deduced there were two additional water molecules attached (the mass of $2H_2O$ = 36 and the charge z = 4 so that 9 × 4 = 36) (Fig. 1*A*). With this information, the exact length of the polymer and the number of sodium ions can be determined by enumeration of all possible combinations. The combination having the closest m/z match can be identified by comparing simulated oligomers with the experimentally observed oligomer based on the average m/z value and the isotope distribution pattern (Fig. 1*B*). The observed m/z values coincide with the simulated m/z values within about 0.15 m/z (< 30 ppm). This remarkable agreement as well as that of the close agreement of the isotope pattern gives us confidence in the assignment of these peaks to polymers of the nucleic acid monomers linked together by phosphodiester bonds (PDBs). Apart from the fully condensed peak of uridylic acid U_{43} [U_{43}-$(H_2O)_{42}$], MS also captured the partially condensed prepolymer peak U_{43}-$(H_2O)_{40}$, suggesting that an incomplete U_{41} polymer is present with two additional UMP molecules adhering by noncovalent binding.

The influence of wet–dry cycle numbers on the oligomer abundance was further investigated by taking UMP as an example. Mass spectra of UMP samples that went through 0 to 3 wet–dry cycles revealed the stepwise generation of long-chain polymers until the third wet–dry cycle (Fig. 2*A*). Of special interest is the so-called 0 wet–dry cycle in which the monomer is sprayed into the mass spectrometer for analysis. At first, it might be supposed that only the monomer would be observed. On the contrary, marked amounts of dimers were present, and as the top panel of Fig. 2*A* reveals, we observed small amounts of U_{38} and U_{39}. This high degree of polymerization provides an important clue concerning the mechanism of polymerization, which will be discussed later. It needs to be recognized that just by forming microdroplets, we are achieving extensive polymerization. It might be wondered whether the oligomerization of nucleic acid monomers by droplet spraying without any wet–dry cycling is an artifact caused by impurities. Two mixtures composed of AMP and UMP and of CMP and GMP were investigated to rule out false positive results. We found the heterogenous dimers AU and CG can be successfully detected after being directly sprayed into the high-resolution MS (*SI Appendix*, Fig. S3), although the intensities are relatively lower than what is found when the mixture goes through the wet–dry cycling process.

There were also different trends of abundance for varied oligomer lengths. The monomer and dimer abundances decreased with the wet–dry cycle at the beginning (Fig. 2*B*), whereas the oligomer and polymer abundance gradually increased (Fig. 2 *C*–*E*), consistent with a gradual elongation process of the nucleotide chain. Two cycles can make the oligomer abundance of middle and long chains reach a maximum. Thereafter, the abundance of those middle and longer oligomers started to decrease but the monomer and dimers' abundances recovered. It was found that hydrolysis and possible degradation became more determinant factors in the third wet–dry cycle. Nonetheless, there was still a proportion of oligomers and polymers surviving and accumulating from the repeated wet–dry cycles. Similar trends of changes with the repeated wet–dry cycles were also observed from the other types of purine and pyrimidine nucleotides.

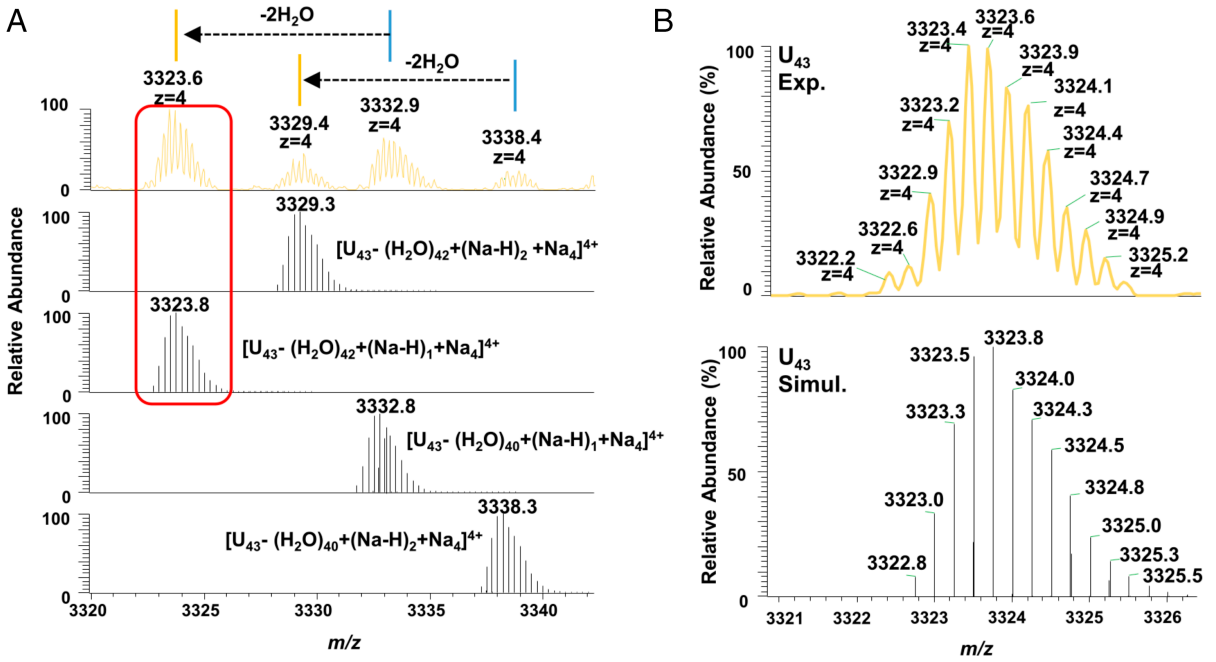

Fig. 1. Polymer identification by nESI–MS. (*A*) A set of ion clusters associated with the 43-mer of uridylic acid, U_{43}, in the mass spectrum. (*B*) The simulated and observed mass spectrum for the U_{43} ion. The mass spectra are an average of 50 or more scans.

The abundance distributions of oligomers resulting from four types of nucleotides (AMP, UMP, dAMP, and TMP) after two wet–dry cycles were examined by nESI–MS. Using ion intensity as a parameter, we found that the abundance of different lengths of nucleotides depended on not only their base composition but also the pentose structure. For instance, ribonucleotides typically polymerized into longer chains than deoxyribonucleotides. The former has a maximum length of 50 nucleotides (Fig. 3*A*), whereas the latter was 25 nucleotides with only sparse detection of longer chains (Fig. 3*B*). Compared to purine nucleotides (AMP, dAMP), pyrimidine nucleotides (UMP, TMP) tended to form relatively longer chains. In mass spectra, there was more than one ion cluster representing a single-length polymer chain because of differences in the number of bound sodium ions. Therefore, we also counted the number of ion clusters for each length of polymer in performing a statistical analysis of their occurrence frequency. The conclusion was consistent with the abundance of nucleotide polymer chains described earlier, that is, the two RNA nucleotides have a higher frequency of longer chains. The average and one SD of (U_n) and (A_n) lengths are 16.3 ± 10.5 and 14.7 ± 9.3, respectively (Fig. 3 *C* and *D*). In contrast, the two DNA nucleotides, $(dTMP)_n$ and $(dAMP)_n$, have relatively shorter chain lengths at 12.1 ± 5.3 and 9.1 ± 3.9 (Fig. 3 *E* and *F*). The intensities of different lengths only represent an approximate estimate of the abundances with the assumption that different lengths have the same ionization efficiency.

Nanopore Sequencing. Nanopore sequencing offered a second independent method for analyzing polymers at the level of single molecules. The sequencing results reported here were performed with a PromethION instrument (Oxford Nanopore Technologies). For monomers, we chose to use deoxythymidine monophosphate (dTMP), a binary mixture of thymidine monophosphate and deoxyadenosine monophosphate (dTMP + dAMP, 1:1 mole ratio), and a third mixture of all four mononucleotides of DNA: dTMP, deoxyadenosine monophosphate, deoxyguanosine monophosphate, and deoxycytidine monophosphate (dTMP + dAMP + dGMP + dCMP, 1:1:1:1 mole ratio). The total concentration of nucleotides was 10 mM in water. The sample was exposed to two wet–dry cycles with durations of 30 min in each dry phase. Because the only components in the initial mixture were mononucleotides, it was not necessary to purify polymer products because the enzymatic steps used to prepare them for sequencing ignore mononucleotides.

As controls, the same mixture of all four mononucleotides was prepared but with the addition of oligomers 27 and 54 nucleotides in length in order to be certain that sequencing would detect known oligomers. The two preparations were not exposed to wet–dry cycles but were sequenced directly. We examined hundreds of successful reads in both controls, and most contained the sequence of either the 27-mer or 54-mer in addition to the adapter. The oligomers are single-stranded. This confirms that the PromethION can sequence short, single-stranded oligomers of DNA. None of the reads matched possible sequences of biological contaminants nor were homopolymers present. This confirmed that the oligomers observed by MS were not from contamination.

PromethION sequencing of cycled mixtures was repeated twice with similar results. Table 1 shows the total number of reads in the first run. The number of reads for each sample ranged from 1,075 to 3,180. Of these, 2 to 3% passed the quality control to be sequenced, and the total number of bases in those reads ranged from 100,000 to 300,000. The percentage passing quality

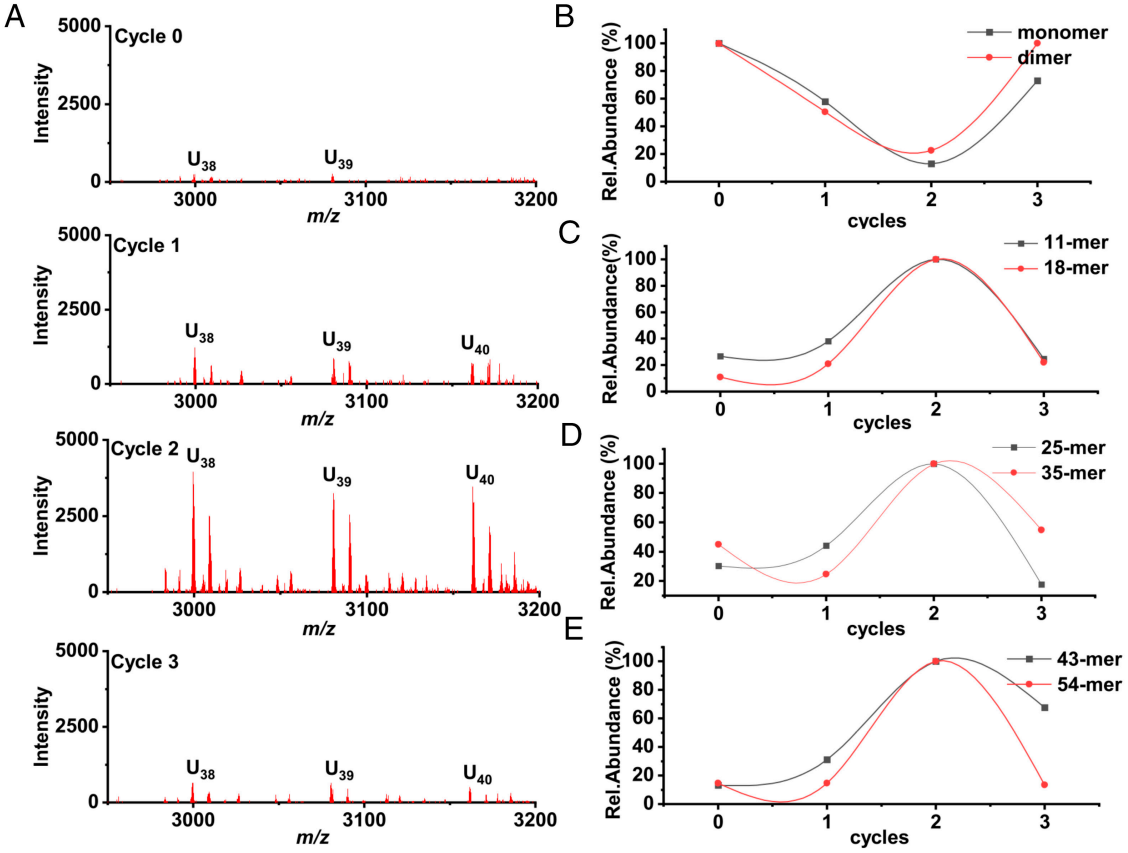

Fig. 2. Nucleotide polymer abundance distribution and changes with the number of wet–dry cycles. (*A*) Representative mass spectra of UMP solution that have gone through 0 to 3 wet dry cycles; (*B–E*) Uridine monomer, dimer, and representative medium, and long chain uridine polymers' abundance change. The mass spectra are an average of 50 or more scans.

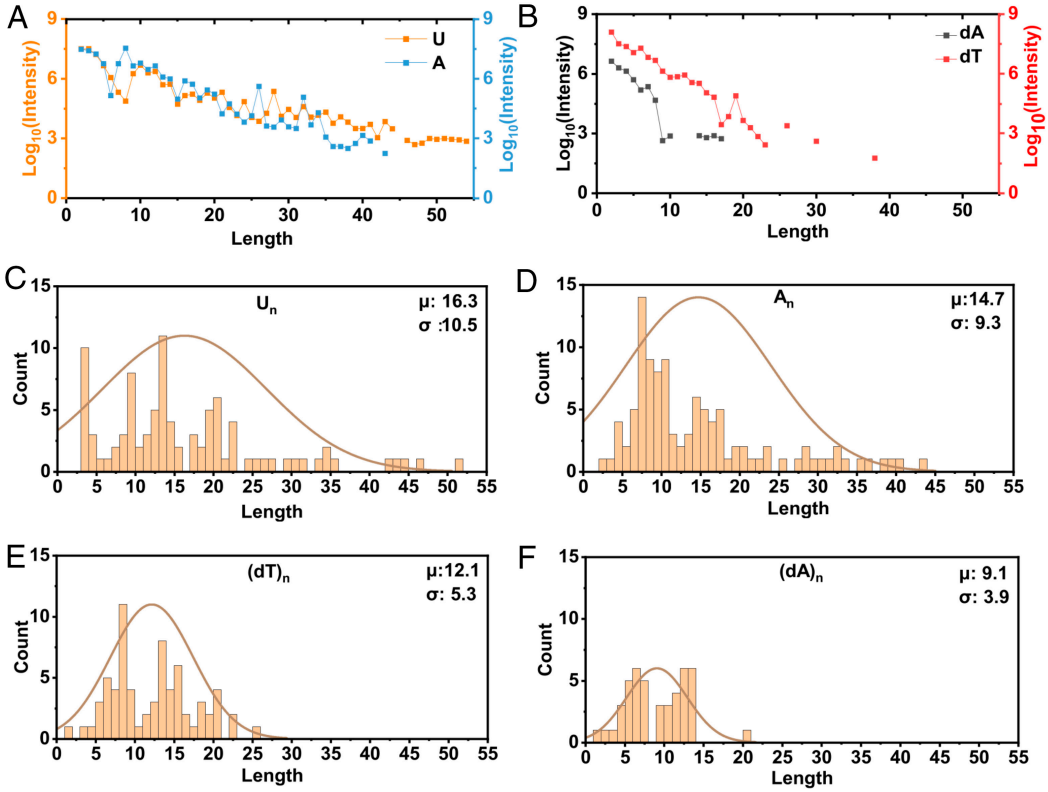

Fig. 3. The net increase in the length of different nucleotide polymers after two wet–dry cycles. (*A*) Abundance distributions of two types of ribonucleic acids; (*B*) Abundance distributions of two types of deoxyribonucleic acids; (*C–F*) The net increases in different lengths of nucleotide polymers after two wet–dry cycles. The μ and σ represent the average and SD in length of the polymer and their values are presented in each panel.

control might seem small, but it should be kept in mind that the polymerization process was spontaneous and not under enzymatic control. If this were occurring in prebiotic conditions on early Earth, the oligomers would be a mixture of lengths and compositions, so these numbers would seem to be a reasonable simulation of the kinds of polymers that might have been present.

The algorithm used for base calling by PromethION software was trained on biological DNA synthesized by polymerase enzymes. The process does not detect single bases passing through the pore. Instead, it monitors picoamp changes in the ionic current as groups of 5 bases, called Kmers, are advanced one base at a time through the pore by a helicase motor. We observed that base calling is sensitive to slight chemical and physical differences in the polymers synthesized by wet–dry cycling when compared to biological DNA. Even though base calling was possible, there was a certain amount of "noise" present in the sequences. However, successful sequencing could be recognized by the fact that DNA adapters are ligated to the strands during preparation. These serve to guide the strand to the nanopore and initiate base calling including the attached adapter strand. The adapter sequence is 5' CCTGTACTTCGTTCAGTTACGTATTGCT-3, so we chose to use a 9-base sequence in the adapter as a marker for a successful read: CCTGTACTT.

This tactic allowed us to search through thousands of reads to find base sequences in the synthetic strands. The presence of the marker increases confidence that the synthetic strand to which it is attached is read correctly. Table 2 presents the nanopore sequencing results for TMP, TMP + dAMP, and a mixture of all four nucleotides. Although most sequences were too long to be resolved by MS, some of the oligomers synthesized from TMP were in the range of those capable of being identified by MS. For example, the oligomers with lengths of 19, 20, 21, 22, and 26 nucleotides found by nanopore sequencing (*SI Appendix*, Table S1) match the MS result of the same lengths shown in Fig. 3*B*.

The oligomers synthesized from the mixture of TMP and dAMP were surprising. Instead of the expected random mix of both nucleotides, the products were mostly homopolymers of TMP or dAMP with the two oligomers occasionally linked into a hybrid polymer. When the number of bases in the homopolymers were counted, the number of TMP nucleotides was three times that of the dAMP homopolymers. For unknown reasons, the marker did not remain attached to some of the polymers in the mixture of TMP + dAMP, so only the base sequences are shown. When four nucleotides were present in the mixture, short oligomers were composed of a seemingly random mix of all four as expected, together with longer homopolymers of dAMP and TMP. There were no homopolymers of dGMP and only a few dC homopolymers.

We summarized the nanopore sequencing results as follows:

1. If TMP is present in solution as a monomer, long homopolymers of oligoT are synthesized by wet–dry cycling.
2. If both TMP and dAMP are present in solution, the products are homopolymers, sometimes linked to each other.
3. When all four bases were present, short sequences were composed of the expected random mixture of bases, whereas other sequences were again homopolymers of dAMP, TMP, and dCMP. There were no homopolymers of dGMP even though G was identified in the mixed sequences.
4. Long sequences composed of repeating base pairs were often present. These are most likely an artifact of the process by which the helicase advances the strand through the nanopore.

Table 1. Quality control of base calling

Sample Name	Number of Reads	Percentage of Passing Reads	Number of Passing Bases
AT-NoFFPE*	1,075	3.0%	0.1 Mb
ATCG	1,876	2.6%	0.3 Mb
ATCG-NoFFPE	1,427	2.5%	0.2 Mb
T	3,180	2.3%	0.3 Mb
T-NoFFPE	1,787	2.0%	0.2 Mb

*FFPE is a kit that is often used to improve sensitivity when sequencing small quantities of biological DNA. It is a mixture of enzymes that repair nicks in dsDNA and prepare the ends of the strands so that a polyA tail can be added for adapter ligation. Sample summary statistics computed by NanoStats using NanoComp to compare multiple samples. (https://github.com/wdecoster/nanocomp)

Discussion

Life did not begin in laboratory conditions featuring purified reactants and water. Instead, the conditions would be "messy" environments such as the subaerial hot spring conditions that we have proposed as plausible sites for life's origin (8). We have therefore explored conditions of prebiotic analog sites such as hydrothermal fields associated with volcanic land masses. The water of a typical hydrothermal field featuring hot springs is distilled from neighboring seawater and falls as precipitation. Unlike salty seawater, the concentration of ionic solutes is typically in the millimolar range or less. Furthermore, aqueous pools in hydrothermal fields are not stable but instead undergo cycles of evaporation and rehydration. As a result, they exist in a steady state in which the products of one reaction become reactants in the next cycle. This state is particularly important if the desired products are polymers with the potential to have functions related to living systems.

In the research described here, we have simulated such wet–dry cycles and investigated polymerization reactions in which the monomers are mononucleotides. In contrast to earlier studies that used imidazole esters of mononucleotides as activated reactants, we found that the concentrating effect of evaporation at an elevated temperature of 85 °C combined with acid catalysis at the water–solid interface provided sufficient activation energy to support the synthesis of ester linkages. This temperature was chosen to reflect the typical of hot springs associated with volcanic activity today, as well as global temperature estimates for early Earth (9). Previous studies have confirmed that dinucleotides are readily synthesized when cyclic 2′-3′-GMP is exposed to drying for several hours together with longer products ranging up to 10 nucleotides in length (10). Earlier research reported that much longer oligomers in the range of 10 to over a hundred nucleotides in length can be synthesized from ordinary mononucleotides by wet–dry cycles simulating those of hydrothermal fields (11–13). The present study employing mass spectrometric analysis and nanopore sequencing has confirmed that wet–dry cycling of ordinary mononucleotides can synthesize oligonucleotides. The presence of PDB was also confirmed by ^{31}P NMR (^{31}P-NMR) and Fourier transform infrared spectroscopy (FTIR). The weak peak with −1.15 (for PolyA) and −0.87 (for PolyU) were successfully detected in the ^{31}P-NMR spectra, matching the chemical shift of phosphorus in PDB (*SI Appendix*, Fig. S4). Additionally, the increased absorption of symmetric and asymmetric PO_2 stretching vibration at 1065 ± 10 cm^{-1} and 1225 ± 10 cm^{-1} were observed in the FTIR spectrum (*SI Appendix*, Fig. S5).

Nanopore Sequencing. We further conducted the nanopore sequencing analysis of polymers synthesized by wet–dry cycling of mononucleotides and detected thousands of sequences emerging from the cycled mixtures. This confirmed the MS conclusion that oligomers had been synthesized. Furthermore, they were recognized by a ligase enzyme that attached an adapter sequence for nanopore sequencing and also recognized by the helicase that controlled the rate at which the oligomer was translocated through the pore. The attachment of the adapter allowed us to search through the sequences, looking for the adapter sequence as a marker for a successful read. Those reads generally matched

Table 2. Typical examples of base calling

Starting	Sample Sequence - Adapter Marker Sequence (bold)	Length
TMP alone	TTTTTTTTTTTTTTTTTTTTTTTTTTTTTTTTTTTTTTTTTTTTTTTTTTTTTTTTTTTTTTTTTTTTTTTTT**CCTGTACTCT**	73 nt
	TTTTTTTTTTTTTTTTTTTTTTTTTTTTTTTTTTTTTTTTTTTTTTTTTTTTTTTTTTTTTTTTTTTTTTTTTTTTTTTTTTTTTTTTTTTTTTTTTTTTTTTTTTTTTTTTTTTTTTTTTTTTTTTTTTTTTTTTTTTTTTTTTTTTT**CCCTGTACT**	149 nt
	TTTTTTTTTTTTTTTTTT**CCCTGTACT**	18 nt
	TTTTTTTTTTTTTTTTTTTTTTT**CCTGTACT**	23 nt
	TTTTTTTTTTTTTTTTTTTTTTTTTTTTTTT**CCTGTACT**	31 nt
	TTTTTTTT**CCCTGTACT**	8 nt
TMP + dAMP (1:1 mixture)	AAAAAAAAAAAAAAAAAAAAAAAAAAAAAAAAAAAAAAAAAAAAAAAAAAAAAAAAAAAAAAAAAAAAAAAAAAAAAAAAAAAAAAAAAAAAAAAAAAAAAAAAAAAAAAAAAAAAAAAAAAAAAAAAAAAAAAAAAAAAAAAAAATTT**CCTGTACT**	144 nt
	TTTTTTTTTTTTTTTTTTTTTTTTTTTTTTTTTTTTTTTTTTTTT**CCCTGTACT**	45 nt
	AAAAAAAAAAAAAAAAAAAAAAAAAAAAAAAATTTTTTTTTTTTTTTTTTTTTTTTTTTTTTTTTTTTTTTTTTTTTTTTTTTTTTTTTTTTTTTTTTTTTTTTTTTTTTTTTTTTTTTTTTTTTTTTTTTTTTTTTTTTTTTTT	167 nt
	TTTTTTTTTTTTTTTTTTTTTTTTTTTTTTTTTTTTTTTTTTTTTTTTTTTTTTTTTTTTTTTTTTTTTTTTTTTTTTTTTTTTTTTTTTTTTTTTTTTTTTTTTTAAAAAAAAAAAAAAAAAAAAAAAAAAAAAAAAAAAATAAAAAAAAAAAAAAAAAAAA	161 nt
dAMP, TMP, dGMP, dCMP (mixture, equal amounts)	TTGCCCTTCTTACTTCGTTCAGTTACATATCTAGGAATGGTTGTT **CCTGTACT**	45 nt
	CTTATTTTTTTATTTTTTTATTTTGTACATCTCCTTATTCCTATAT **CCTGTACT**	46 nt
	TTGATCTTACTTCGTTCAGTTCTT**CCTGTACT**	24 nt

expectations from the composition of the mononucleotides. There were also some surprises. Nanopore sequencing was developed to read double-stranded biological DNA, but we observed many oligoT sequences synthesized from TMP alone even though they would be single-stranded. Apparently, they were ligated to the adapter sequence and then found the nanopore for the helicase to advance the strand through the pore. The base calling algorithm developed for double-stranded biological DNA could recognize oligomers of TMP and dAMP if they were attached to the adapter sequence but also produced sequences without the adapter that did not make sense. Future research may help us to understand why this is happening.

Because nonenzymatic polymerization produces complex mixtures of multiple products varying in length, MS can only identify shorter oligomers composed of single nucleotides such as those described here. In contrast, nanopore sequencing resolves individual molecules which allows longer polymers to be characterized in terms of length, base composition, and sequence. These physical and chemical properties provide a powerful test of the nature of the polymers:

1. To be translocated through a nanoscopic pore, the polymers must be linear with no branching. This is true of all reads without regard to passing quality control for base calling.
2. The polymers must have a diameter slightly smaller than the diameter of the nanopore. This allows the polymer to be drawn through the nanopore while monitoring the ionic current that is used to identify the bases.
3. The polymers must be polyanions so that the electrical field in the pore can capture them from the solution and then exert an electrophoretic force that drives them through.
4. Several enzymes are used to prepare the polymers for sequencing. These include a repair enzyme and an end prep enzyme used to modify the end of the strand to undergo ligase-catalyzed attachment to the adapter DNA that guides the strand to the nanopore.
5. A helicase is used to control the rate at which the strand moves through the nanopore at ~450 bases per second.
6. Even though the synthetic strands are advanced through the nanopore, there are apparently minor differences in their chemical and physical properties that can confuse the base calling algorithm.

All three of the samples contained polymers that met the above criteria. The numbers of reads varied from ~1,000 to ~3,000 depending on the sample (Table 1). If these criteria are met, it is reasonable to assume that the system of enzymes used to prepare DNA for sequencing recognizes the strands as equivalent to biological DNA.

Mechanism of Ester Bond Synthesis. It is important to note that most biochemical reactions in the laboratory are performed in dilute aqueous solutions with enzymes and chemically activated reactants such as nucleoside triphosphates. Such conditions follow the usual laws of thermodynamics and kinetics, but the conditions described here are very different. To understand how polymerization can occur during wet–dry cycling, it is necessary to realize that the system goes through a stage in which the reactants are exposed to interfaces such as air–water interfaces of microdroplets or the extremely concentrated solute molecules in a drying film (14–18). Previous studies have shown that many chemical reactions can be vastly accelerated under conditions that are not thermodynamically possible in dilute aqueous solutions (19–21).

Several features lead to this unexpected behavior. Whereas bulk water has a homogeneous distribution of H^+ and OH^- ions arising from the autoionization of water surrounded by water solvation shells, water in contact with a hydrophobic medium, such as air or an insoluble solid, shows a strong propensity to be acidic on its surface, that is, to show a large H^+ concentration (22). This fact can be seen, for example, in the ability of water droplets to resemble magic acid and capture carbocations that otherwise have only a fleeting existence (23). Previously, others have noted that water's acidity at the interface can be a controlling factor in causing oligomerization to occur (24, 25). We propose that an acid-catalyzed nucleophilic attack of a ribose –OH group on the phosphate of a neighboring nucleotide causes oligomerization to occur (26). To test whether glass is catalyzing the oligomerization process, we replaced the borosilicate glass slide with a Teflon plate for the same wet–dry cycling procedure. The heterogenous dimers AU and CG can still be detected by the high-resolution mass spectra after the wet–dry cycling of two mixtures composed of AMP and UMP and of CMP and GMP. There is no apparent decrease of the dimer peak intensities in the Teflon group compared to the borosilicate glass slide group (*SI Appendix*, Fig. S6).

Furthermore, the concentrated monomers serving as condensation reactants and the loss of water molecules (as the condensation product) from the confined phase of a drying film, will disrupt the usual equilibrium and drive the condensation reaction toward polymerization. Moreover, positive and negative ions will have different affinities for hydrophobic versus hydrophilic phases, leading to a charge separation and the formation of an electric double layer at the interface (27–29). This fact causes a strong electric field to develop at the interface that can align reagents and drive reactions that cannot occur in the bulk liquid (30, 31). Such fields also cause extensive alignment of water molecules as observed by Zhou et al. (32).

An important distinction is that three-dimensional solvation of ions in which the ions are surrounded by water molecules on all sides cannot happen at the interface. Instead, only partially solvated ions are present which markedly changes the reactivity. Thus, when a thin film of reactants becomes anhydrous, monomers are immobilized and unable to undergo extensive polymerization, but at interfaces produced during a wet–dry cycle, the conditions can promote rapid and extensive polymerization, which is what we have observed in this study.

Another consideration is that the film of reactants may not be disordered glass. Instead, order can emerge during evaporation, just as crystals appear when a dilute solution evaporates. Himbert et al. used X-ray diffraction to investigate dried films of a mixture of adenosine monophosphate and UMP (33). The diffraction patterns gave a clear indication of the 3.4 Å spacing expected if linear arrays of the nucleotides had assembled by base stacking. Such hidden order would help overcome the entropy barrier of an otherwise disordered glassy state, thereby promoting the ability of condensation reactions to link the stacked nucleotides by PDB.

Stability and Degradation. It is well known that conditions of acidic pH and elevated temperature promote several reactions that tend to degrade both nucleotides and their polymers. Hydrolysis of the ester bonds linking nucleotides in nucleic acids is a random process that occurs continuously. Given time, hydrolysis of ester bonds would completely degrade polymers to their component nucleotides. However, hydrolysis occurs at a certain rate, and if polymer synthesis is taking place at a faster rate, the result will be a steady state in which polymers can exist. The synthesis of oligomers described here occurs rapidly within a few minutes, but the hydrolysis rate is much slower, with half-times measured

in days (34). This difference in rates accounts for the fact that oligomers accumulate during wet–dry cycling.

A second hydrolysis reaction is depurination which causes purine bases like adenine to be released from the N-glycoside bond to ribose or deoxyribose. We do observe partial depurination in the MS analysis for both the AMP and dAMP. This phenomenon is more apparent in a low pH like 2.5 (*SI Appendix*, Fig. S7). Mungi et al. employed MS to discover depurination of dimer and trimer products during wet–dry cycling (35). This result might lead to the conclusion that large polymers of mononucleotides cannot be synthesized by wet–dry cycling. However, the results reported here show that long strands of intact RNA and DNA oligomers are present in the mixture. We believe that this difference arises from the reaction conditions. Mungi et al. used 2.5 mM disodium salts of nucleotides and reduced the pH to 2.0 with sulfuric acid, whereas we prepared 10 mM nucleotides in their acid form so that the pH was 2.5 without addition of a strong acid that would become highly concentrated during evaporation.

Hydrothermal Fields Are Conducive to Polymer Synthesis. A fair question concerns a source of mononucleotides that can serve as monomers. Powner and Sutherland (36, 37) were first to address this question from the perspective of organic chemistry, and Becker et al. made further progress by incorporating wet–dry cycles (38). A future research goal will be to combine mononucleotide synthesis with polymerization reactions such as those described here as a model for investigating the origin of nucleic acids in hydrothermal ponds. In conclusion, the studies presented here demonstrate that wet–dry cycling on early Earth seems a plausible source for forming nucleic acid oligomers needed in evolving from nonlife to life.

Data, Materials, and Software Availability. All study data are included in the article and/or *SI Appendix*.

ACKNOWLEDGMENTS. We are grateful to Gerald Joyce for his critical reading of an earlier draft of this manuscript that helped us strengthen the arguments presented, and Miten Jain for helping us to analyze the results of nanopore base calling. P.S. acknowledges the financial support provided by the Baltic-American Freedom Foundation and Research Council of Lithuania, agreement No. S-PD-24-69. R.N.Z. and X.S. also acknowledge the support from the US Air Force Office of Scientific Research through the Multidisciplinary University Research Initiative program (AFOSR FA9550-21-1-0170). D.D. thanks Joshua Gardner and Ivo Violich for performing nanopore sequencing of samples and Karen Miga for making a PromethION available for this research. We also thank Wasatch Biolabs for expert sequencing of control samples.

1. T. Inoue, L. E. Orgel, A nonenzymatic RNA polymerase model. *Science* **219**, 859–862 (1983).
2. J. P. Ferris, Mineral catalysis and prebiotic synthesis: Montmorillonite-catalyzed formation of RNA. *Elements* **1**, 145–149 (2005).
3. M. Morasch, C. B. Mast, J. K. Langer, P. Schilcher, D. Brau, Dry polymerization of 3′,5′-cyclic GMP to long strands of RNA. *Chem. Bio. Chem.* **15**, 879–883 (2014).
4. C. Obianyor, G. Newnam, B. Clifton, M. Grover, N. V. Hud, Impact of substrate-template stability, temperature, phosphate location, and nick-site base pairs on non-enzymatic DNA ligation: Defining parameters for optimization of ligation rates and yields with carbodiimide activation. Bio. Rxiv [Preprint] (2019). https://www.biorxiv.org/content/10.1101/821017v1 (Accessed 7 November 2024).
5. R. Krishnamurthy, N. V. Hud, Introduction: Chemical evolution and the origins of life. *Chem. Rev.* **120**, 4613–4615 (2020).
6. D. S. Ross, D. W. Deamer, Dry/wet cycling and the thermodynamics and kinetics of prebiotic polymer synthesis. *Life* **6**, 28 (2016).
7. D. S. Ross, D. W. Deamer, Prebiotic oligomer assembly: What was the energy source? *Astrobiology* **19**, 517–521 (2019).
8. B. Damer, D. Deamer, The hot spring hypothesis for an origin of life. *Astrobiology* **20**, 429–452 (2020).
9. L. P. Knauth, D. R. Lowe, High Archean climatic temperature inferred from oxygen isotope geochemistry of cherts in the 3.5 Ga Swaziland Supergroup, South Africa. *GSA Bull.* **115**, 566–580 (2003).
10. A. V. Dass *et al.*, RNA oligomerisation without added catalyst from 2′,3′-cyclic nucleotides by drying at air-water interfaces. *Chem. Sys. Chem.* **5**, 1–8 (2023).
11. I. A. Chen, P. Walde, From self-assembled vesicles to protocells. *Cold Spring Harb. Perspect. Biol.* **2**, 002170 (2010).
12. S. Rajamani *et al.*, Lipid-assisted synthesis of RNA-like polymers from mononucleotides. *Orig. Life Evol. Biosph.* **38**, 57–74 (2008).
13. V. De Guzman, H. Shenasa, W. Vercoutere, D. Deamer, Generation of oligonucleotides under hydrothermal conditions by non-enzymatic polymerization. *J. Mol. Evol.* **78**, 251–262 (2014).
14. Y. Li, X. Yan, R. G. Cooks, The role of the interface in thin film and droplet accelerated reactions studied by competitive substituent effects. *Angew. Chem. Int. Ed.* **55**, 3433–3437 (2016).
15. Z. Wei, M. Wleklinski, C. Ferreira, R. G. Cooks, Reaction acceleration in thin films with continuous product deposition for organic synthesis. *Angew. Chem. Int. Ed.* **129**, 9514–9518 (2017).
16. R. M. Bain, C. J. Pulliam, F. Thery, R. G. Cooks, Accelerated chemical reactions and organic synthesis in Leidenfrost droplets. *Angew. Chem. Int. Ed.* **55**, 10478–10482 (2016).
17. A. M. Deal, R. J. Rapf, V. Vaida, Water–air interfaces as environments to address the water paradox in prebiotic chemistry: A physical chemistry perspective. *J. Phys. Chem. A* **125**, 4929–4942 (2021).
18. E. C. Griffith, A. F. Tuck, V. Vaida, Ocean–atmosphere interactions in the emergence of complexity in simple chemical systems. *Acc. Chem. Res.* **45**, 2106–2113 (2012).
19. I. Nam, J. K. Lee, H. G. Nam, R. N. Zare, Abiotic production of sugar phosphates and uridine ribonucleoside in aqueous microdroplets. *Proc. Natl. Acad. Sci. U.S.A.* **114**, 12396–12400 (2017).
20. I. Nam, H. G. Nam, R. N. Zare, Abiotic synthesis of purine and pyrimidine ribonucleosides in aqueous microdroplets. *Proc. Natl. Acad. Sci. U.S.A.* **115**, 36–40 (2018).
21. D. T. Holden, N. M. Morato, R. G. Cooks, Aqueous microdroplets enable abiotic synthesis and chain extension of unique peptide isomers from free amino acids. *Proc. Natl. Acad. Sci. U.S.A.* **119**, 2212642119 (2022).
22. M. de la Puente, D. Laage, How the acidity of water droplets and films is controlled by the air-water interface. *J. Am. Chem. Soc.* **145**, 25186–25194 (2023).
23. A. Kumar, S. Mondal, S. Banerjee, Aqueous microdroplets capture elusive carbocations. *J. Am. Chem. Soc.* **143**, 2459–2463 (2021).
24. S. Ishizuka, A. Matsugi, T. Hama, S. Enami, Chain-propagation, chain-transfer, and hydride-abstraction by cyclic carbocations on water surfaces. *Phys. Chem. Chem. Phys.* **20**, 25256–25267 (2018).
25. S. Ishizuka *et al.*, Controlling factors of oligomerization at the water surface: Why is isoprene such a unique VOC?. *Phys. Chem. Chem. Phys.* **20**, 15400–15410 (2018).
26. H. Kaddour, N. Sahai, Synergism and mutualism in non-enzymatic RNA polymerization. *Life* **4**, 598–620 (2014).
27. C. F. Chamberlayne, R. N. Zare, Simple model for the electric field and spatial distribution of ions in a microdroplet. *J. Chem. Phys.* **152**, 184702 (2020).
28. C. F. Chamberlayne, R. N. Zare, J. G. Santiago, Effects of weak electrolytes on electric double layer ion distributions. *J. Phys. Chem. Lett.* **11**, 8302–8306 (2020).
29. C. F. Chamberlayne, R. N. Zare, What role does the electric double layer play in redox reactions at planar electrostatically charged insulating surfaces? *Top. Catal.* **65**, 228–233 (2022).
30. H. Xiong, J. K. Lee, R. N. Zare, W. Min, Strong electric field observed at the interface of aqueous microdroplets. *J. Phys. Chem. Lett.* **11**, 7423–7428 (2020).
31. H. Hao, I. Leven, T. Head-Gordon, Can electric fields drive chemistry for an aqueous microdroplet? *Nat. Commun.* **13**, 1–8 (2022).
32. Z. Zhou, X. Yan, Y. H. Lai, R. N. Zare, Fluorescence polarization anisotropy in microdroplets. *J. Phys. Chem. Lett.* **9**, 2928–2932 (2018).
33. S. Himbert, M. Chapman, D. W. Deamer, M. C. Rheinstadter, Organization of nucleotides in different environments and the formation of pre-polymers. *Sci. Rep.* **6**, 31285 (2016).
34. M. Oivanen, S. Kuusela, H. Lonnberg, Kinetics and mechanisms for the cleavage and isomerization of the phosphodiester bonds of RNA by Brönsted acids and bases. *Chem. Rev.* **98**, 961–990 (1998).
35. C. V. Mungi, N. V. Bapat, Y. Hongo, S. Rajamani, Formation of abasic oligomers in nonenzymatic polymerization of canonical nucleotides. *Life* **9**, 57 (2019).
36. M. Powner, B. Gerland, J. Sutherland, Synthesis of activated pyrimidine ribonucleotides in prebiotically plausible conditions. *Nature* **459**, 239–242 (2009).
37. N. J. Green, J. Xu, J. D. Sutherland, Illuminating life's origins: UV photochemistry in abiotic synthesis of biomolecules. *J. Am. Chem. Soc.* **143**, 7219–7236 (2021).
38. S. Becker *et al.*, Unified prebiotically plausible synthesis of pyrimidine and purine RNA ribonucleotides. *Science* **366**, 76–82 (2019).